

# Influence Of Dewaxing on Mechanical properties of kapok fiber-reinforced polymer composite

Ramyaranjan Das<sup>1</sup>, C Dash<sup>2</sup>, P Behera<sup>3</sup> and Dillip Kumar Bisoyi<sup>\*</sup>

<sup>1, \*</sup>Department of Physics and Astronomy, National Institute of Technology, Rourkela, Sundargarh, India, 769008

Corresponding author's e-mail address- [dkbisoyi@nitrkl.ac.in](mailto:dkbisoyi@nitrkl.ac.in)

**Abstract.** The low density, lightweight, easy processing and biodegradability nature of Natural fiber-reinforced polymer composite have gained enough attention from many researchers and scientists. Kapok Fiber (*Ceiba pentandra*) is a natural cellulosic fiber have a hollow microtubular structure and a high degree of hollowness. The hand lay-up technique has been adopted for kapok fiber-reinforced epoxy polymer composite fabrication with different fiber loading(2, 3, 4, 5, 6 and 7 wt %). The mechanical strength of kapok fiber-reinforced polymer epoxy composite is investigated through the flexural and tensile test. The best flexural and tensile performance is observed at 5 wt% loading of kapok fiber. To increase compatibility between fiber and epoxy matrix dewaxing process is adopted. The effect of dewaxing on cellulose crystallinity, crystallinity size, surface morphology, elemental composition and functional groups of fiber are studied. The roughness of the fiber surface increases after dewaxing due to the partial removal of non-cellulosic compounds like lignin, pectin, wax and some oily substances. The increase in fiber surface roughness and cellulose crystallinity index by chemical treatment made a strong interlocking at the fiber-matrix interface. The effect of dewaxing on mechanical strength is also studied to fabricate the composite for the benefit of society.

**Keywords:** Composite; Kapok Fiber; Matrix; Dewaxing Process.

## 1. Introduction

Natural plant fibers have gained enough attention from many researchers and scientists because of their low cost, easy availability, low fiber density, thermal, low energy consumption, and electrical insulating nature. The natural fiber is chosen over synthetic fiber for its eco-friendly nature, biodegradability, and non-toxic nature. Nowadays, Both environmental legislation and consumers are shifting towards greener technology. As reported earlier, biodegradable composites are prepared with lignocellulosic fibers such as luffa, hemp, straw, coir, jute, flax, and abaca[1]. Natural fiber-reinforced composites are widely used in domestic, automobile, sports, aerospace, and thermal and electrical insulating equipment like door panels, bath tops, chairs, railing, swimming pool insulating taps, switchboards, and power lines, etc. [2]. Natural fiber-reinforced polymer composites show good mechanical strength and do not pose any severe health-related hazards while processing compared to synthetic fiber. Synthetic fiber-reinforced composites produce some toxic gases which cause dermal or respiratory irritation. The adverse effect of petroleum-based product consumption, plastics, synthetic fiber, glass fiber and carbon fiber may be responsible for environmental pollution and the greenhouse effect[3]. Natural fiber-reinforced composites are low cost, easy to process, and environment friendly, making them more fascinating. The addition of plant-based fiber to a polymer matrix helps in two ways. First, it enhances composite properties and Second, it reduces composite costs [4]. Kapok fibers are obtained from seed pods of the kapok tree, consisting of around 53% cellulose, 30% hemicelluloses, 21% lignin, 5% wax and 1% wax[10]. The degradation of hemicelluloses takes place first at around 250 to 300<sup>0</sup>C. The temperature range around 300<sup>0</sup> to 350<sup>0</sup> c is

attributed to cellulose degradation. Complex oxygen containing lignin degrades at about 400<sup>0</sup> to 600<sup>0</sup>C. It is the lightest naturally available lignin-rich plant fiber, consisting of about 80% hollowness. The highest degree of hollowness makes it the best choice for reinforcing material in biodegradable lightweight composite fabrication[10].

## 2. Materials and Methods

Kapok fiber is collected from Baripada local farmers in Odisha, India, with average diameters of 15-20  $\mu\text{m}$ . The fruits of kapok fiber contain kapok husk, seeds and kapok fiber. Fibers are extracted from the fruits followed by surface impurities and lumps from the fiber that are removed manually. Then it is placed inside a vacuum oven at room temperature for 2 hr to remove dust particles. These fibers are named "Raw kapok Fiber" (RKF). Ethanol( $\text{C}_2\text{H}_6\text{O}$ ), Benzene( $\text{C}_6\text{H}_6$ ), Epoxy (L-12) and Hardener (K-6) are collected from Himedia Laboratories Pvt. Ltd, Mumbai.

### 2.1 Dewaxing Process

Kapok fiber contains wax and impurities on the surface, which may affect fiber-matrix interfacial adhesion. Raw Kapok Fibers are purified through the Dewaxing process. The extractor solvent contains ethanol and benzene in the ratio 1:2 taken in a round bottom flask. These two chemicals are introduced to remove fatty substances like pectin, wax and impurities present in the top layer of the fiber. This treatment can also help in surface modification of fiber and better interlock of fiber with the matrix. The extractor apparatus consists of a Heating element, temperature variator, round bottom flask containing solvent and kapok fiber, a thermometer for temperature measurement, and cold water circulation for vapour condensation. Extractor solvent (Benzene and Ethanol) and fiber cooked in the round bottom flask. The cooking process is done with consecutive 2 hr heating and 2 hr cooling up to 12 hr. The temperature inside the flask is maintained between 30°-65° celcius. After 12 hr, fibers are extracted from the flask, and washed thoroughly in tap water, followed by deionized water. Finally, these fibers are soaked in an oven at a temperature 80° for 24 hr and are named "Dewaxed kapok fiber" (DKF).

### 2.2 Composite Fabrication

After pretreatment on kapok fibers, the hand lay-up method is used for composite fabrication. This method is adopted for its low cost and easy processing features. A rectangular glass mold of dimension (170×110×5)  $\text{mm}^3$  is prepared for composite fabrication. The matrix is placed under a high-intensity ultrasonic processor (Ultrasonic processor Sonopros, PR-1000M) for 1 hr to get a homogeneous mixture and break complex epoxy bonds. Then the matrix is degassed in a vacuum oven for 6 hr at 80°c temperature to make it bubble-free. 10:1 weight ratio of Epoxy (L-12) with hardener is taken and stirred for 5 min to form a matrix. The hardener accelerates the curing process. The fibers are chopped into small pieces of 1 to 3 mm and mixed with epoxy to create a blend. The blend is stirred continuously for 5 min to get a uniform mixture and then poured into the mold. A releasing agent, heavy-duty silicon spray is applied over the glass mold to remove the composite slab easily. The whole blend is laminated with a releasing plastic sheet, and special care has been taken to make it free from bubbles and homogeneous using an iron roller. The entire arrangement is loaded to remove excess resin, and air bubbles[5]. Finally, the specimen composite is removed from the glass mold after 24 hr and cut into the required dimensions using a zig saw machine blade for the mechanical test.

## 3. Instrumentation for characterization.

### 3.1 Contact angle (CA) measurement

The CA between fiber liquid interface is determined with a CA apparatus (Kruss DSA 25, Germany). Hydrophobicity of the fiber depends upon the Contact angle formed by water at the fiber, water and air phase boundary. The hydrophobicity of the fiber is directly proportional to the Contact angle. The interaction of liquid at the solid surface can be explained by the youngs equation, and it is given by  $\gamma^{sv} = \gamma^{sl} + \gamma^{lv} \cos \theta$  .....(1)

Where  $\gamma^{sv}$  is the surface tension at solid- the vapour interface,  $\gamma^{sl}$  is the surface tension at the solid-liquid interface and  $\gamma^{lv}$  is the surface tension at the liquid-vapour interface.

The accumulation of energy and imbalance force at the interface of two phases is known as interfacial surface tension. The cohesive force between the molecules of the same type of substance gives rise to surface tension. When adhesive strength between two phases increases, the material diverts from hydrophobicity. From equation (1), the cosine angle of contact at the fiber water interface is given by

$$\cos \theta = \frac{\gamma^{sv} - \gamma^{sl}}{\gamma^{lv}} \dots\dots\dots(2)$$

When  $\gamma^{sv} > \gamma^{sl}$ ,  $\cos \theta$  is +ve and  $\theta < 90^\circ$ , which indicates the material is to be hydrophilic.

When  $\gamma^{sv} < \gamma^{sl}$ ,  $\cos \theta$  is -ve and  $\theta > 90^\circ$ , which indicates the material is to be Hydrophobic.

### 3.2 X-Ray Diffraction(XRD)

The XRD spectra of RKF and DKF are obtained by X-ray diffractometer (Ultima IV –Rigaku, Japan) with a generator functioning at 40 kV voltage and 40 mA current. The intensity of the diffracted radiation is measured from  $5^\circ$ - $55^\circ$  with a scan rate of  $5^\circ/\text{min}$  and a step size of  $0.05^\circ$ .

The crystallinity index of the fiber is estimated using Segal's maximum peak intensity formula. Segal's empirical formula is given by

$$(CrI) = \left( \frac{I_{002} - I_{am}}{I_{002}} \right) \times 100 \dots\dots\dots(3)$$

Where  $I_{002}$  corresponds to the intensity of cellulose peak and  $I_{am}$  corresponds to the intensity of amorphous material. The crystallinity size is estimated using Scherrer's formula

$$(CrS) = \frac{k\lambda}{\beta \cos \theta} \dots\dots\dots(4)$$

Where  $k$  is Scherrer's constant (Dimensionless shape factor which is equal to 0.94).  $\lambda$  is the wavelength of the incident X-ray source ( $1.54\text{\AA}$ ).  $\theta$  is the peak position that corresponds to the maximum intensity of diffraction radiation.  $\beta$  is the full width half maximum

### 3.3 Morphological study of kapok fiber by SEM

Scanning electron microscopy (SEM) is a non-destructive surface analysis technique used to study sample dimension, surface roughness and surface defects of the samples. The present study examines the surface morphologies and the surface defects of kapok fibers by SEM (JEOL JSM-6480 LV, Japan) at 20kV.

An Energy dispersive x-ray spectrometer (EDX) attached to the scanning electron microscope performed the elemental analysis of raw and dewaxed fibers.

### 3.4 Fourier Transform Infrared Spectroscopy

FTIR spectra of RKF and DKF were recorded on FTIR spectrometer (Perkin Elmer spectrum, US) using KBr pellets. Fiber samples are grounded into powder form, mixed with KBr binder, and pressed into pellet form using a Hydraulic press. The average percentage of raw and dewaxed kapok fiber transmittance is recorded in the near-infrared region, within the wavelength range  $4000\text{-}400\text{ cm}^{-1}$ .

### 3.5 Mechanical Properties Analysis

Flexural Test and Tensile test estimates the mechanical properties of kapok fiber reinforced composites at different fiber loading. Both flexural and tensile tests are executed in a Universal Testing Machine (UTM Instron-5967, UK) with an environmental chamber at  $30^\circ\text{C}$  by applying a crosshead speed of  $2\text{mm}/\text{min}$ . In order to evaluate mechanical properties, composites are cut into the dimensions  $(90 \times 12 \times 5)\text{mm}^3$  for flexural tests and  $(170 \times 22 \times 5)\text{mm}^3$  for tensile tests according to the ASTM standard of D-7254 and D-3039, respectively. The flexural strength of the sample is estimated using the following formula

$$(\sigma) = \frac{3 \times F \times L}{2b \times d^2} \dots\dots\dots(5)$$

Where  $\sigma$  is the Flexural Strength (in MPa),  $F$  is the load at the fracture point,  $b$  is the width (in mm),  $d$  is the thickness (in mm), and  $L$  is the span length.

The maximum tensile strength is estimated using the following formula

$$(\sigma_t) = \frac{F_t}{b \times d} \dots \dots \dots (6)$$

where  $F_t$  is the maximum load(in MPa) at the fracture point, b is the width(in mm) of the composite, and d is the thickness(in mm) of the composite.

## 4. Results and discussion

### 4.1 Hydrophobicity of the fiber testing by Contact angle (CA) measurement

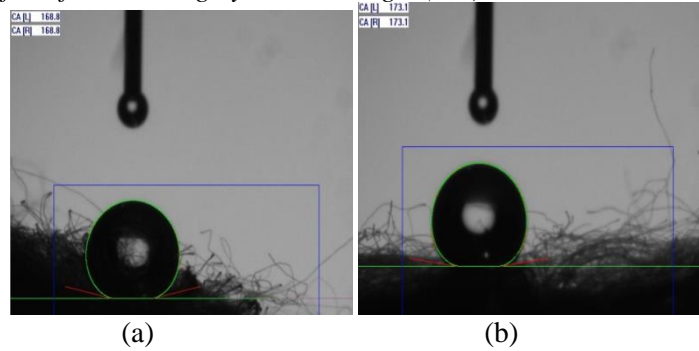


**Figure 1.** Contact angle measurement of kapok fiber (a)RKF (b) DKF

The hydrophobic nature of kapok fiber is confirmed by the CA measurement experiment. The contact angle of the fiber is measured by dropping deionized water droplets on flattened kapok fiber bundles. The interaction of water at raw and Dewaxed kapok fiber surfaces is shown in Figures 1(a) and 1(b), respectively. In the case of RKF, the contact angle is found to be 168.8°. In DKF, the contact angle of interaction is found to be 173.1°, which indicates the increase in hydrophobicity of the kapok fiber surface in the dewaxing process. This is due to an increase in surface roughness.

### 4.2 X-Ray Diffraction(XRD)

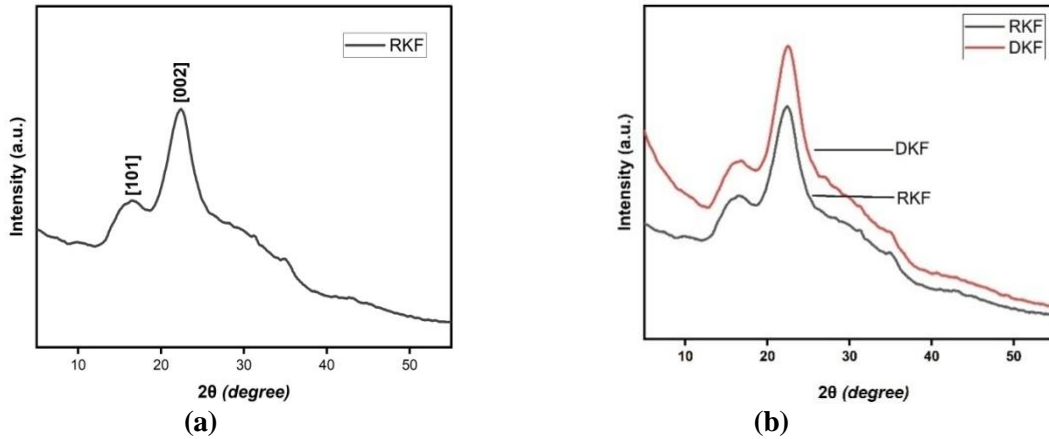


**Figure 2.** XRD Pattern of Kapok Fiber (a) RKF (b) Both RKF and DKF

Both RKF and DKF exhibit a similar kind of diffraction pattern. The XRD patterns of RKF and DKF are shown in figure 5. The main characteristic peaks of RKF appear at Braggs diffraction angles 22.42° and 16.68°. The non-cellulosic amorphous peak, i.e. the minimum intensity between the valley region of two cellulose crystalline peak, appear at 18.62°. The relative percentage of crystallinity and crystallinity size of both RKF and DKF are listed in Tables 1. and 2. Respectively.

**Table 1.** The relative percentage of crystallinity of both RKF & DKF

Sample name	$I_{002}$	$I_{am}$	CrI(%)
	$= I_{cr}$		

<b>RKF</b>	8181.33	4353.83	46.78
<b>DKF</b>	10626.38	5554.18	47.73

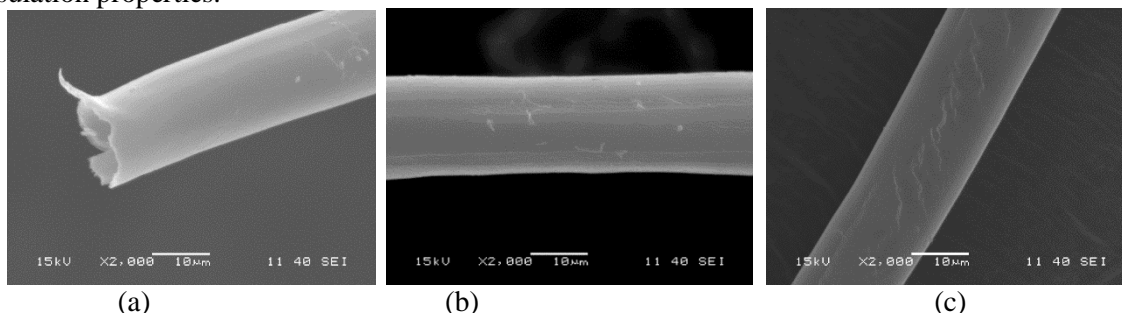
**Table 2.** Crystalline size of both RKF and DKF

Sample name	$\beta$ =FWHM (in degree)	$\theta$ = Braggs diffraction angle corresponds to maximum intensity (in degree)	$CrS$ = crystallinity size (in nm)
<b>RKF</b>	12.72	11.21	2.49
<b>DKF</b>	11.67	11.21	3.01

The dewaxing treatment removes the amorphous phase, i.e. the wax and surface impurities from the kapok fiber surface. The removal of the amorphous phase leads to an increase in crystallinity index and crystallinity size. Table 2 shows that  $\beta$  the value of the cellulose peak decreases in the dewaxing process. The decrease in ( $\beta$ ) value leads to an increase in crystallinity size. The increase in crystallinity size corresponds to an increase in the degree of crystallinity[6]. The Dewaxing process removes the impurities and wax, which causes swelling of the crystalline region[7]. The crystal distortion and defects decrease due to the regular arrangement of the crystal chain.

#### 4.3 Morphological study of kapok fiber by SEM

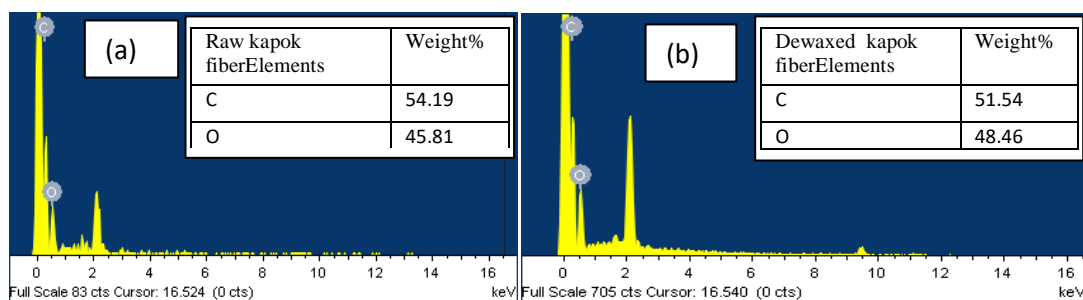
The SEM morphology of kapok fiber in figure 3. (a) shows that it has a thin wall, large lumen, tubular structure and a high degree of hollowness. Due to the high degree of hollowness, it has thermal insulation properties.



**Figure 3.** SEM micrographs of kapok fibers: (a) hollow structure of kapok fiber, (b) Raw kapok fiber, (c) Dewaxed kapok fiber.

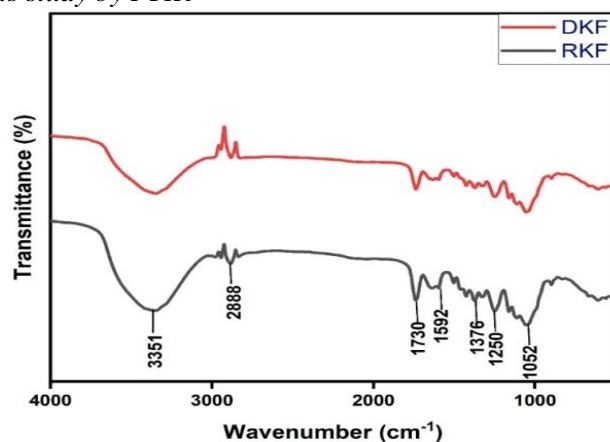
Figure 3.(b) shows SEM images of raw kapok fiber. The smoothness of the kapok fiber is due to the presence of lignin pectin and wax. It can be seen that the surface roughness and diameter of kapok fiber are changed after purification. The average diameter of the kapok fibers is found to be  $17\mu m$  and it decreases after dewaxing treatment due to the increase in surface wrinkles and removal of surface wax and impurities. After purification of fiber, the average diameter of the fibers is found to be  $15\mu m$ . Figure 3.(c) shows SEM images of dewaxed kapok fibers. The roughness of the fiber surface increases after dewaxing due to the partial removal of lignin, pectin, wax and some oily substances present on the surface of kapok fibers.

Figure 4. Shows EDAX Spectra and elemental composition of Raw and dewaxed Kapok fiber. The EDAX analysis shows that kapok fiber mainly consists of carbon and oxygen due to its cellulose structure. Fiber samples are platinum coated to promote the emission of secondary electrons and make them conductive. The extra peak at 2.1 keV of both RKF and DKF is due to platinum coating, which was cancelled out later for elemental calculation. After dewaxing treatment, the carbon percentage of the fiber decreases, and the oxygen percentage increases. The O/C ratio in dewaxed kapok fiber increases to 0.94 from 0.85. The increase in oxygen percentage in dewaxed kapok fiber is due to the partial removal of higher carbon-containing Wax and some surface impurities[8].



**Figure 4.** EDAX Spectra of kapok fiber (a) RKF (b) DKF

#### 4.4 Chemical components study by FTIR



**Figure 5.** RKF and DKF – FTIR Spectrum

Figure 5. shows the FTIR spectra of untreated and dewaxed kapok fiber. The middle infrared region ( $4000\text{--}400\text{ cm}^{-1}$ ) of the spectra is divided into two regions. The wavenumber associated from  $4000$  to  $1500\text{ cm}^{-1}$  is set for the diagnostic region, where the  $1500$  to  $400\text{ cm}^{-1}$  region is associated with the fingerprint region. The major peaks of RKF that appears in diagnostic regions are  $3351\text{ cm}^{-1}$ ,  $2888\text{ cm}^{-1}$ ,  $1730\text{ cm}^{-1}$  and  $1592\text{ cm}^{-1}$ . The peak around  $3351\text{ cm}^{-1}$  is assigned to  $\text{--OH}$  stretching due to the cellulose component whose intensity peak reduces in the case of dewaxed kapok case. It indicates the loss of  $\text{--OH}$  groups from the fiber structure upon the treatment. The peak at  $2888\text{ cm}^{-1}$  corresponds to asymmetric and symmetric  $\text{CH}_2$  and  $\text{CH}_3$  stretching and confirms the presence of wax which later reduces due to dewaxing treatment. The transmission peak at  $1730\text{ cm}^{-1}$  is the characteristic of hemicellulose and is attributed to  $\text{C=O}$  stretching whose transmission peaks are again reduced by dewaxed fiber. The weak peak at  $1592\text{ cm}^{-1}$  assigns to  $\text{C=C}$  skeletal vibration due to the  $\text{C=C}$  aromatic ring of lignin. The peak at  $1376\text{ cm}^{-1}$  is assigned to  $\text{--CH}_3$  asymmetric and  $\text{C-H}$  symmetric deformation of lignin which later becomes very insignificant in the dewaxed case. The peaks around  $1250\text{ cm}^{-1}$  are attributed to  $\text{C-O}$  bending associated with lignin and hemicellulose whereas  $1062\text{ cm}^{-1}$  assigns to  $\text{C-O-C}$  stretching due to the presence of carbohydrate and polysaccharides in cellulose. The dewaxing treatment of the kapok fiber is observed to be lower in transmittance intensities indicating the partial removal of wax, pectin, hemicellulose and other impurities. The FTIR peaks and their corresponding functional groups are listed in table 3.

**Table 3.** FTIR peaks and corresponding functional groups

FTIR spectral peak (in $\text{cm}^{-1}$ )	Description
<b>3351</b>	$\text{--OH}$ group stretching
<b>2888</b>	$\text{CH}_2$ and $\text{CH}_3$ stretching

<b>1730</b>	C=O stretching
<b>1592</b>	C=C skeletal vibration
<b>1376</b>	-CH <sub>3</sub> asymmetric and C-H deformation
<b>1250</b>	C-O bending
<b>1062</b>	C-O-C stretching

#### 4.5 Mechanical Properties Analysis

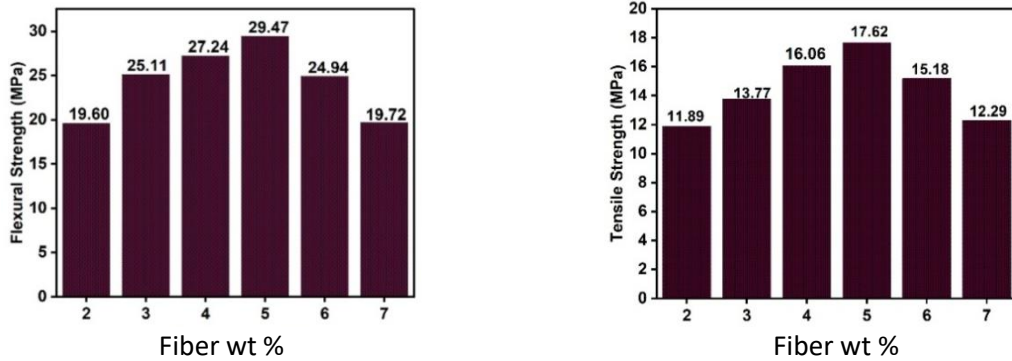


**Figure 6.** (a) Flexural Strength of RKFRC (b) Tensile Strength of RKFRC

Figure 6. shows the effect of fiber loading on flexural and tensile strength of both raw kapok fiber-reinforced polymer composite. The incorporation of fiber with the epoxy resin is taken at different weight percentages (2-7 wt%). An increasing pattern of both flexural and tensile strength of composites is observed with an increase in fiber loading. The rising pattern of mechanical strength is observed from 2-5%, which may be due to the increase in bond interlocking between fiber and matrix. Beyond 5% weight loading, the mechanical strength of the composites decreases, which may be due to the nonuniform stress transfer at fiber- matrix interface and increase in void content. At 5% loading, the better performance in flexural and tensile strength is observed due to the uniform stress transfer between the fiber-epoxy interface and proper wetting. At 5% fiber loading, the flexural and tensile strength of the composite is found to be 29.47 MPa and 17.62 MPa, respectively.

#### 4.6 Effect of Dewaxing on Mechanical Strength of the Composite

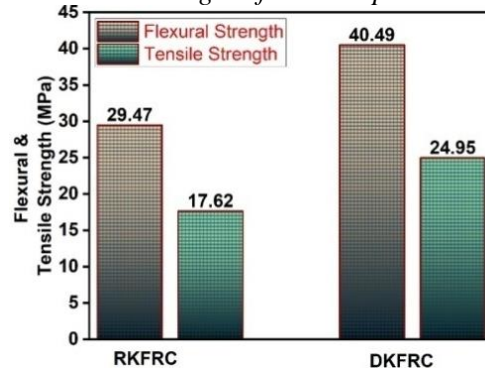


**Figure 7.** Mechanical strength of raw and dewaxed kapok fiber-reinforced composite

Figure 7. shows the effect of dewaxing on the mechanical strength of kapok fiber-reinforced composite at optimal fiber loading i.e. 5%. A significant increase in the mechanical strength of the composite is observed after dewaxing. The flexural and tensile strength of the composites increases by 37.41% and 31.62%, respectively. Mechanical strength of the dewaxed kapok fiber-reinforced composite increases due to the increase in surface roughness of the fiber, crystallinity index and Crystallinity size[9]. The removal of surface impurities and wax from fiber increases the compatibility between fiber and epoxy.

## 5. Conclusion

The present study is concerned with the effect of dewaxing on the mechanical strength of composites. Kapok fiber-reinforced composites are fabricated using the hand lay-up technique. The Dewaxing process partially removed surface impurities, wax, oily substances and pectin. At 5 wt% optimal fiber loading, the best mechanical strength of the composite is obtained. At optimal fiber loading, the Flexural and tensile strength of the composite is found to be 29.47 MPa and 17.62 MPa, respectively. After dewaxing mechanical strength of the composite increases due to the removal of surface impurities, increase in crystallinity index and surface roughness. So to achieve composites with desired properties, interfacial interaction between fiber and matrix must be good. We can produce a polymer composite with desired properties by choosing an appropriate combination of kapok fiber and epoxy.

## References

- [1] Pai, A. R., & Jagtap, R. N. (2015). Surface morphology & mechanical properties of some unique e natural fiber reinforced polymer composites—A review. *Journal of materials and environmental science*, 6(4), 902-917.
- [2] Holbery, J., & Houston, D. (2006). Natural-fiber-reinforced polymer composites in automotive applications. *Jom*, 58(11), 80-86.
- [3] ]Bisoyi, D. K., Oram, S. K., & Dash, C. (2021). A mechanical and dielectric study on calcium hydroxide pre-treated kapok husk-reinforced epoxy composites. *Polymer Bulletin*, 1-17.
- [4] Mittal, V., Saini, R., & Sinha, S. (2016). Natural fiber-mediated epoxy composites—a review. *Composites Part B: Engineering*, 99, 425-435.
- [5] Dash, C., Das, A., & Kumar Bisoyi, D. (2020). Influence of pretreatment on mechanical and dielectric properties of short sunn hemp fiber-reinforced polymer composite in correlation with fine structure of the fiber. *Journal of Composite Materials*, 54(23), 3313-3327.
- [6] Dash, C., & Bisoyi, D. K. (2021). Study on Dielectric and charge transport behavior in alkali-treated randomly oriented Sunn Hemp Fiber Reinforced epoxy composite in connection with the microstructure of fiber. *Journal of Natural Fibers*, 1-16.
- [7] Chen, X., Gu, L., Dang, C., & Cao, X. (2022). A lightweight and high-strength epoxy composites based on graphene oxide modified kapok fibers. *Composites Communications*, 31, 101111.
- [8] Borsoi, C., Ornaghi Jr, H. L., Scienza, L. C., Zattera, A. J., & Ferreira, C. A. (2017). Isolation and characterization of cellulose nanowhiskers from microcrystalline cellulose using mechanical processing. *Polymers and Polymer Composites*, 25(8), 563-570.
- [9] Sabarinathan, P., Rajkumar, K., Annamalai, V. E., & Vishal, K. (2020). Characterization on chemical and mechanical properties of silane treated fish tail palm fibres. *International Journal of Biological Macromolecules*, 163, 2457-2464.
- [10] Draman, S. F. S., Daik, R., Latif, F. A., & El-Sheikh, S. M. (2014). Characterization and thermal decomposition kinetics of kapok (*Ceiba pentandra* L.)-based cellulose. *BioResources*, 9(1), 8-23.